Talanta 253 (2023) 123940

Contents lists available at ScienceDirect

Talanta

journal homepage: www.elsevier.com/locate/talanta

Aggregation-aided SERS: Selective detection of arsenic by surface-enhanced Raman spectroscopy facilitated by colloid cross-linking

Moumita Das [a,b,**], Debraj Gangopadhyay [b,*], Radek Pelc [b], Romana Hadravová [b], Jaroslav Šebestík [b], Petr Bouř [a,b,***]

[a] Department of Analytical Chemistry, Faculty of Chemical Engineering, University of Chemistry and Technology, Technická 5, 16628 Prague 6, Czech Republic
[b] Institute of Organic Chemistry and Biochemistry, Czech Academy of Sciences, Flemingovo náměstí 2, 16610 Prague 6, Czech Republic

ARTICLE INFO

Keywords:
Arsenic detection
Surface-enhanced Raman scattering
Silver nanoparticles
Colloid cross-linking

ABSTRACT

Arsenic of natural or industrial origin often occurs in water and makes it impotable. Due to its high toxicity, very sensitive detection is required. In the present study an ultra-sensitive arsenite (As^{3+}) sensing is reported, based on aggregation-aided surface-enhanced Raman scattering (AA-SERS) of modified silver colloids. SERS intensity of mercapto-compounds attached to the colloidal silver nanoparticles surface is greatly increased in the presence of arsenic. Colloid aggregation is facilitated by cross-linking; a meshwork consisting of arsenic atoms and glutathione bridges is formed, as indicated by UV–Vis absorption spectroscopy, TEM and Raman imaging. The best 2-mercaptopyridine reporter molecule makes it possible to directly detect As^{3+} at concentrations as low as 0.5 ppb, which is better than achieved by the SERS technique so far.

1. Introduction

Arsenic is a toxic element responsible for a multitude of diseases if found in food or beverages [1–11]. According to the World Health Organization (WHO) a concentration as low as 10 ppb (μg L^{-1}) in drinking water may be dangerous to humans [1,12]. However, arsenic-contaminated water is often used, e.g., for irrigation, and arsenite anions can spread and accumulate in the crops. Its toxicity has been attributed to arsenic thiol affinity as it dehydrogenates the SH group in proteins, enzymes, etc., which results in cell death [13–16]. Life-threatening medical conditions caused by contaminated water have been reported in many countries in the Indian peninsula, south-east Asia, or South America [17–21]. In most European countries, arsenic concentration in natural water sources are mostly below the WHO limit. Higher levels in groundwater have been reported from certain regions of Italy, Poland and Hungary [22–31]. In the USA, 7% of wells suffer from arsenic levels above 10 ppb [32].

Due to its high toxicity, very sensitive detection of arsenic is necessary. Several protocols have been reported so far, including surface-enhanced Raman scattering (SERS) [1,22,33–43]. In SERS, the Raman signal is enhanced by several orders of magnitude upon adsorption of the molecules of interest on metal surfaces [44–49]. Being one of the most sensitive spectroscopic tools, the SERS technology is also widely used in environmental studies. It can trace a wide range of inorganic and organic molecules, including DNA, RNA, proteins, peptides [15,36,44,50,51], or even living cells [52]. Other techniques that can be used for arsenic detection and provide comparatively the same sensitivity include mass spectrometry, atomic fluorescence spectrometry, and nuclear magnetic resonance spectroscopy. The main advantages of SERS are simplicity, it is time and cost-effective, and requires reasonable effort for the sample preparation. It requires small amount of sample and is effective for selective as well as mixture analysis. However, SERS experiments are often not well reproducible. In the present work we therefore aim at a SERS protocol which is both reproducible and could

Abbreviations: **SERS**, **surface-enhanced Raman scattering**; **AgNPs**, **silver nanoparticles**; **GSH**, **glutathione**; **2-MPY**, **2-mercaptopyridine**; **4-MPY**, **4-mercaptopyridine**; **2-MP**, **2-mercaptopyrimidine**; **TEM**, **transmission electron microscopy**.

* Corresponding author.
** Corresponding author. Department of Analytical Chemistry, Faculty of Chemical Engineering, University of Chemistry and Technology, Technická 5, 16628 Prague 6, Czech Republic.
*** Corresponding author. Department of Analytical Chemistry, Faculty of Chemical Engineering, University of Chemistry and Technology, Technická 5, 16628 Prague 6, Czech Republic.
E-mail addresses: moumita.das@uochb.cas.cz (M. Das), debraj.gangopadhyay@uochb.cas.cz (D. Gangopadhyay), petr.bour@uochb.cas.cz (P. Bouř).

https://doi.org/10.1016/j.talanta.2022.123940
Received 22 July 2022; Received in revised form 26 August 2022; Accepted 14 September 2022
Available online 17 September 2022

achieve low limits of detection.

Greaves and Griffith reported As^{5+} SERS spectra but only at concentrations greater than 100 mg L^{-1}, using Ag sols [53]. Other reports focused on SERS detection of aqueous arsenic samples by monolayers of polyhedral Ag nanocrystals [33]. Compared to three forms of polyvinylpyrrolidone-capped Ag nanoparticles (AgNPs), the monolayer of octahedral AgNPs yielded better results, and exhibited a linear relationship between the SERS signal and arsenic concentration, between 1.0 and 180 ppb. Banerjee's group [54] used gold nanoparticles (AuNPs) and developed a highly sensitive dynamic light scattering (DLS) assay for arsenic sensing in aqueous solution. Other SERS experiments included both As^{5+} and As^{3+} forms [36,55]. On multilayer Ag nanofilm substrates, the detection limit was below 5 ppb. Ag nanowire substrate was also fabricated [22]. These substrates were stable, sensitive, selective and uniform, and yielded reproducible results. Other groups prepared substrates by a modified mirror reaction [55] or electrolytic plating [22]. The presence of electrolytes at low concentrations can considerately improve the SERS sensitivity. Song et al. prepared a biosensor based on Au–Ag core-shell nanoparticles [56]. Li et al. suggested an indirect detection strategy based on glutathione and 4-mercaptopyridine-doped AgNPs [34]. This was then improved to suit quantitative detection of As(III) ions in continuous flow of a microfluidic chip [35]. Liu et al. [57] developed a nanosheet substrate consisting of Ag nanoporous film doped with γ-Fe_2O_3; As(V) could then be detected down to 1 ppb.

Nevertheless, a practical use of the SERS technology brings about many problems. Preparation of a stable, highly functionalized substrate is difficult as impurities and even minor variations of the experimental conditions can strongly affect the spectra.

In the present study, we investigate a more user-friendly method, with arsenic attached to glutathione [47] acting as a 'bridge' molecule. This cross-links the silver nanoparticles into dense colloidal aggregates, and SERS of a 'reporter' molecule (a mercapto-compound [58]) is greatly enhanced. We refer to this phenomenon as 'aggregation-aided SERS' (AA-SERS). Our protocol represents efficient 'direct' sensing of arsenite ion (As^{3+}), it does not rely on data extrapolation employed in other protocols [34,35], and achieves the lowest detection limit reported so far. 2-mercaptopyridine was found as the most efficient reporter molecule. The aggregation is confirmed by Raman microscopy and transmission electron microscopy.

2. Materials and methods

2.1. Preparation of borate-stabilized silver nanoparticles (AgNPs)

Commercial chemicals (Sigma-Aldrich) and Milli-Q water were used throughout. Colloidal AgNPs were synthesized by a standard reduction procedure described elsewhere [59–62]. Solution 'S1' was prepared by mixing 20.5 μL of 0.182 M $AgNO_3$ with 3.73 mL of water. Solution 'S2' consisted of 11.5 μL of 2.01 M $NaBH_4$ in triethylene glycol dimethyl ether and 11.25 mL of water. S1 was added dropwise to S2 under constant stirring continued for another 3 min. The mixture was then filtered through a cotton plug. The filtrate was left overnight at room temperature in dark, and then stored at 5 °C for at least one day before measuring SERS spectra. In the UV–Vis absorption spectra, the AgNPs exhibited an absorption band at 398 nm (full width at half maximum of 98 nm). The synthesized AgNPs showed an enhancement factor of at least 10^4 with 1 mM aqueous solution of 2-MPY, but can be bigger for lower concentrations.

2.2. Modification of AgNPs by bridge and reporter molecules

Modified AgNPs were prepared by mixing 1 mL of the borate-stabilized AgNPs substrate (see above) with 100 μL of 0.5 μM glutathione (GSH, the "bridge" molecule) and 100 μL of 1 μM 2-mercaptopyridine (2-MPY), 4-mercaptopyridine (4-MPY), or 2-mercaptopyrimidine (2-MP), these being the so-called "reporter" molecules. The mixture was vigorously stirred for 2 min and kept overnight at room temperature in dark before recording SERS spectra. We explored also other concentrations of the reporter (mercapto compound) and bridge (GSH) molecules; the composition specified above provided the strongest AA-SERS. Note that GSH links the colloid particles and the As^{3+} ions together but does not provide measurable SERS signal. Higher GSH concentrations than 0.5 μM caused the colloid to immediately precipitate.

2.3. Solutions of As^{3+} and other metal ions for method calibration

As_2O_3 was dissolved in ~10 μL of 0.1 M sodium hydroxide solution (due to poor solubility in pure water), and then diluted with Milli-Q water to achieve As^{3+} concentrations ranging from 0.1 to 500 ppb (μg L^{-1}). Similarly, solutions of Al, Co, Fe, K, Ni, Pb and Zn salts were made. Before SERS measurement, 20 μL of the analyte solution was added to 60 μL of modified AgNPs substrate and left undisturbed for 5 min to let the colloid aggregate.

2.4. SERS measurement

SERS spectra were recorded using a backscattering μ-ChiralRaman-2X™ instrument (BioTools, Inc.) with 532 nm laser excitation and 7 cm^{-1} spectral resolution. The laser power was 300 mW, accumulation time 10 min.

2.5. UV–VISible spectra measurement

UV–VISible spectra of dispersed AgNPs (before and after modification by 2-MPY and GSH) and aggregated AgNPs (after also adding As^{3+}) were measured by a WTW PhotoLab7600 spectrometer. The sample was placed in a quartz cuvette of 1 cm path length, and the spectra recorded between 200 and 900 nm.

2.6. Transmission electron microscopy (TEM)

Parlodion-carbon-coated grids were floated on top of a 10 μL drop of the sample for 5 min. After drying, the grids were examined in a JEOL JEM-1011 electron microscope operated at 80 kV.

2.7. Raman microscopic imaging

SERS image of AgNPs aggregated by the arsenic-glutathione meshwork was captured by a WITec alpha300 R Raman microscope with a Zeiss 100 × /0.9 objective. A square spacer (outer dimensions ca 20 × 20 mm) made of Parafilm M (thickness ca 0.13 mm) was placed on a microslide (Figs. S1–A, Supporting Information). A 5 μL droplet of colloid solution was positioned on the microslide in the middle of the spacer and covered with a standard coverslip (18 × 18 mm, thickness ca 0.17 μm) then clamped to the microslide by stationery or other suitable clips (Figs. S1–B, Supporting Information). The coverslip was sealed around its edges by nail varnish (not visible in the figure) to the microslide to prevent evaporation of the colloid solution. Once the varnish solidified (within a few minutes) the clips were removed (Figs. S1–C, Supporting Information).

A specimen chamber thus made can be used with objectives featuring a working distance of at least ca 0.3 mm (spacer + coverslip thickness). Spectral imaging was carried out in an area of 20 × 20 μm (nominally 40 × 40 pixels, integration time 1 s per pixel) under 532 nm excitation by a diode laser operating at 1 mW.

3. Results and discussion

First, control SERS spectra of 2-MPY, glutathione, and their mixture were measured in arsenic-free solutions (Fig. 1, parts A, B and C, respectively). As apparent, these analytes provide only small band

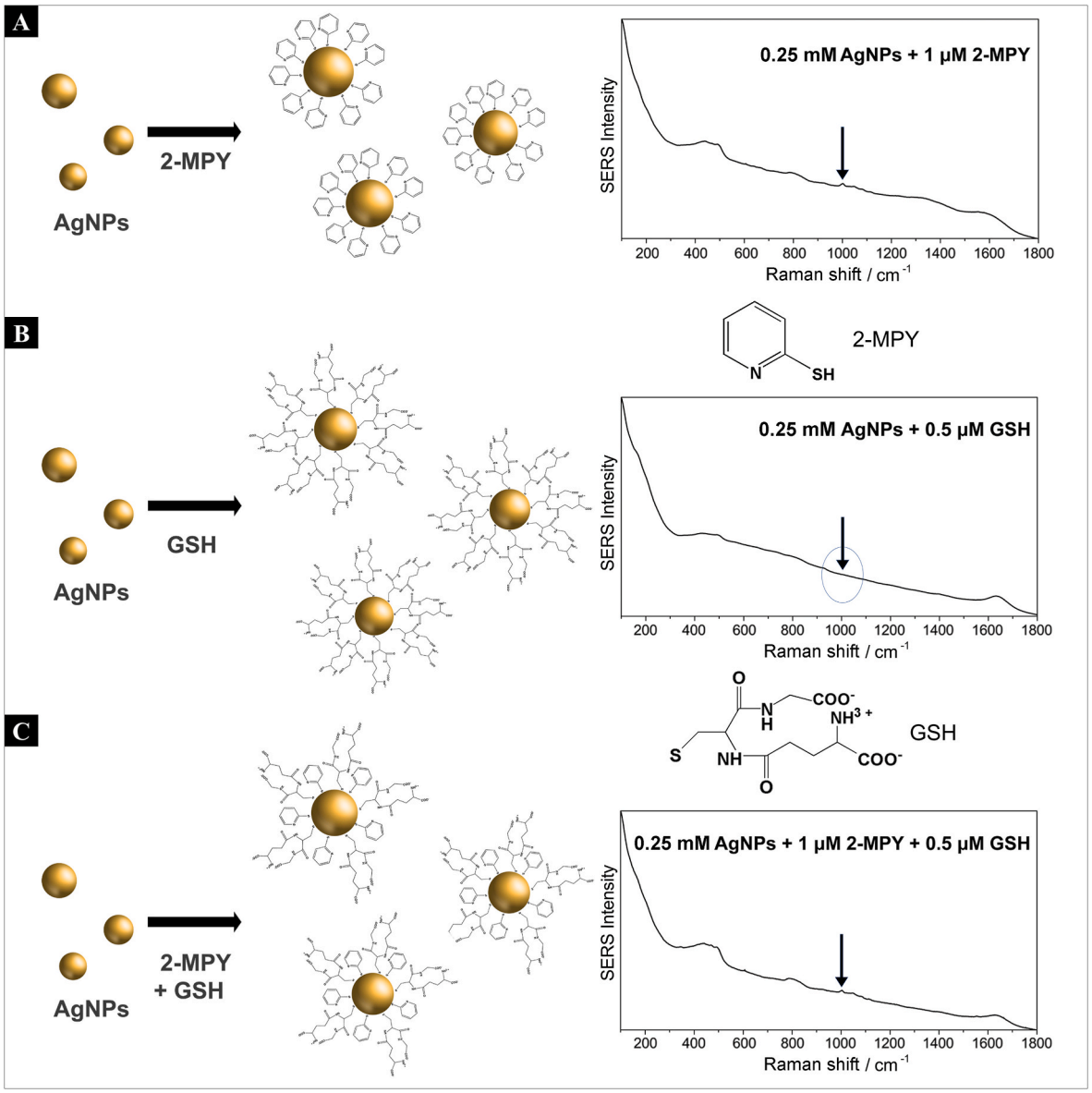

Fig. 1. Surface-enhanced Raman spectra (SERS) of borate-stabilized silver nanoparticles (AgNPs [0.25 mM $AgNO_3$], 1 mL) modified by (A) mercaptopyridine (2-MPY, 100 μL), (B) glutathione (100 μL), and (C) 2-MPY (100 μL) + glutathione (100 μL), at concentrations stated in the figure. Arrows/ellipse in the spectrum indicate the position/absence of the ring breathing band of 2-MPY.

intensities at micromolar concentrations. One can see, for example, an aromatic band around 1000 cm^{-1}, while, except for the background, the spectra are dominated by the glass (~420 cm^{-1}) and water (1650 cm^{-1}) bands.

We explain the lack of strong SERS by incomplete or non-existent aggregation of the colloids. Addition of As^{3+}, however, induces aggregation and a strong SERS signal of 2-MPY appears (Fig. 2), which has already been observed for 4-MPY [34,35].

In order to observe the SERS spectra at very low concentrations of As^{3+}, it is therefore necessary to aggregate the colloids. In aggregates, hotspots are present in which the laser intensity, and consequently the SERS signal is greatly amplified [63,64]. Higher As^{3+} concentration is expected to produce more extensive aggregation of AgNPs, thereby producing stronger SERS.

GSH is a chelating ligand that binds to silver nanoparticle surfaces via Ag–S bonds. This fact is well-known and has been extensively researched. Through an As–S link, also the arsenic may react with mercapto group-containing ligands. In this study, however, after the modification of silver nanoparticles, neither GSH nor the mercapto compound contains a free SH group to interact with the As^{3+} ions. On the other hand, As^{3+} can bind via As–O bonds to three GSH molecules, thus producing the aggregates (Fig. 2B, references [34,35]). This creates sufficient SERS hotspots with increased intensity of the electromagnetic field where the signal from the reporter molecule is enhanced.

The aggregation can also be detected by absorption spectroscopy. Fig. 3 shows UV–Vis absorption spectra of the AgNPs, before and after addition of GSH + 2-MPY, for different concentrations of As^{3+}. As for SERS (Fig. 2), the presence of micromolar amounts of GSH and 2-MPY does not affect the absorption band significantly. However, the extra addition of As^{3+} brings about profound changes; the 410 nm band gets smaller and a new maximum appears at ~540 nm, which is due to AgNP aggregation [65].

Similarly, the aggregation can be observed in the transmission electron microscopic (TEM) images (Fig. 4, Fig. S2, Supporting Information). Micromolar concentrations of GSH and 2-MPY result only in small aggregates of the AgNPs. Presence of As^{3+}, however, brings about much larger clusters, typically ca 1 μm in diameter..

The aggregates were also observed in solution, by both brightfield

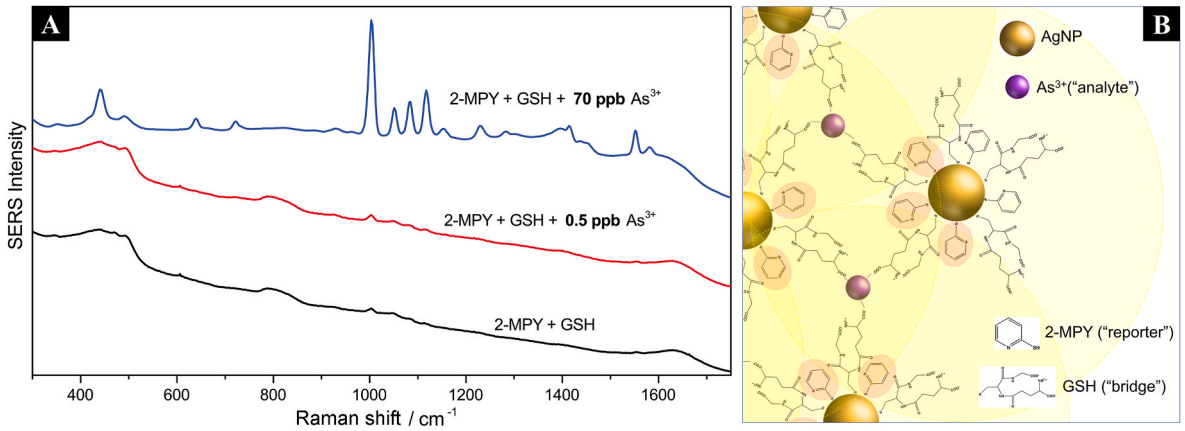

Fig. 2. (A) SERS spectra of a mixture of 2-mercaptopyridine (2-MPY, 1 μM) and glutathione (GSH, 0.5 μM) in the absence and presence of As^{3+} ions. (B) Suggested mechanism of aggregation. Glutathione attached to the silver nanoparticles (AgNPs, from 0.25 mM $AgNO_3$) binds also to arsenic, thus efficiently cross-linking the aggregates into a more densely packed meshwork.

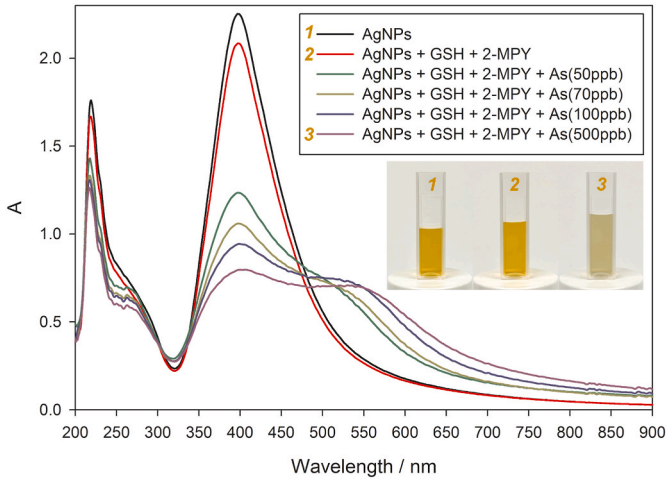

Fig. 3. UV–Vis absorption spectra of silver nanoparticles (AgNPs, nominally 0.25 mM $AgNO_3$) upon successive addition of glutathione (GSH, 0.5 μM), 2-mercaptopyridine (2-MPY, 1 μM) and various concentrations of As^{3+}.

and Raman microscopy (Fig. S1, Supporting Information and Fig. 5, respectively). As expected, higher concentration of As^{3+} generated more aggregates. Raman imaging also revealed that the SERS intensity is stronger in bigger aggregates. It is worth mentioning here that the Raman imaging was done on a WITec alpha300 R Raman microscope, which uses a small laser spot. Unlike the SERS detection experiment, which was done on a BioTools μ-ChiralRaman-2X™ instrument where several aggregates were focused within the laser spot, here the laser spot can be focused at different regions within a single aggregate. That is why a location-specific variation in intensity of the Raman bands could be observed. Raman imaging was done to confirm that the aggregates observed in TEM is not a drying artifact.

The dependence of SERS signal on the As^{3+} concentration is documented in detail in Fig. 6, for all three mercapto-compounds (2-MPY, 4-MPY and 2-MP); an almost linear dependence between As^{3+} concentration and SERS intensity was observed between 10 and 100 ppb. This is documented for the strongest band, the ring breathing mode of pyridine/pyrimidine ring (Fig. 7). Other band assignments are given in Table S1, Supporting Information and the data consisting of calculation of average SERS intensities and standard deviations, plotted in Fig. 7, are presented in Table S2, Supporting Information.

As apparent from Fig. 7, the dependence is more complicated below 10 ppb. For 4-MPY and 2-MP, the intensity is about constant below 3 ppb and 10 ppb, respectively, and then there is a stepwise change. We found that 2-MPY is more sensitive as a SERS reporter compared to 4-MPY and 2-MP, and the linearity in concentration vs intensity plot (Fig. 7) is well-maintained even below 10 ppb all the way down to 0 ppb. We have experimentally observed this effect to be reproducible and could

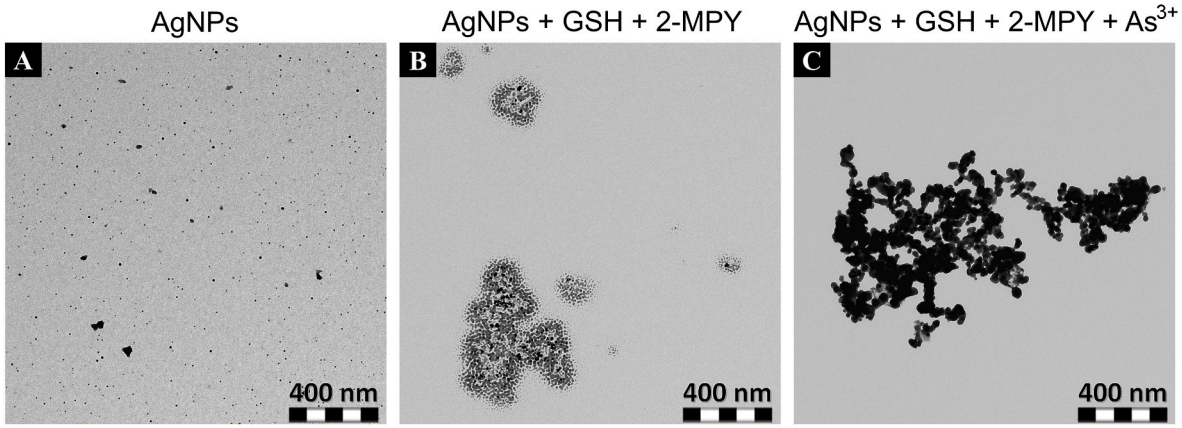

Fig. 4. Visualization of aggregation by transmission electron microscopy. (A) Silver nanoparticles alone (AgNPs, nominally 0.25 mM $AgNO_3$) are barely visible. (B) An addition of glutathione (GSH, 0.5 μM) and 2-mercaptopyridine (2-MPY, 1 μM) brings about partial aggregation. (C) Adding As^{3+} (100 ppb) results in denser and bigger aggregates (cf. Fig. 5). More TEM images are shown in Supporting Information (Fig. S2).

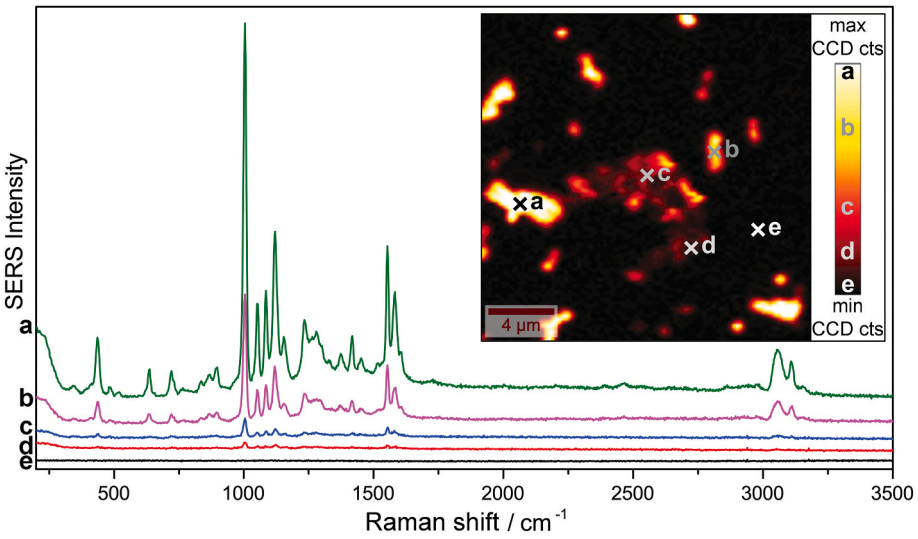

Fig. 5. SERS image of aggregates formed upon mixing silver nanoparticles (AgNPs, nominally 0.25 mM $AgNO_3$), glutathione (GSH, 0.5 µM), 2-mercaptopyridine (2-MPY, 1 µM) and 100 ppb A^{3+} (cf. Fig. 4). SERS spectra (a–c) were obtained from corresponding spots in the image. For brightfield image, see Fig. S1, Supporting Information.

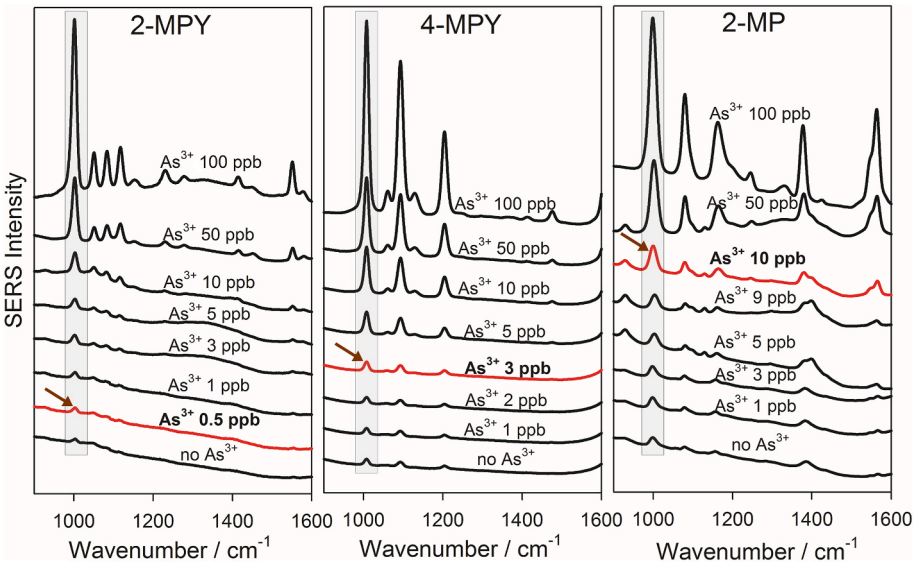

Fig. 6. SERS spectra of three reporter molecules: 2-mercaptopyridine (2-MPY), 4-mercaptopyridine (4-MPY) and 2-mercaptopyrimidine (2-MP), at various concentrations of As^{3+}, and the same concentration of silver nanoparticles (nominally 0.25 mM $AgNO_3$). The ring breathing mode is highlighted. Arrows mark the SERS detection limit for As^{3+} (cf. Fig. 7). All spectra were obtained in the presence of glutathione (GSH, 0.5 µM). More SERS spectra are shown in Supporting Information (Fig. S3).

'directly' detect 0.5 ppb of As^{3+} from the SERS spectrum, without the need of data extrapolation. To the best of our knowledge, this is the lowest detection limit achieved in the realm of SERS. The obvious reason why 2-mercaptopyridine is the best reporter is unknown. We suggest that it is a combination of molecular reactivity and symmetry, determining the SERS response. In all our experiments, the standard deviation of the blank signal is practically zero. Therefore, any signal higher than the blank signal may be considered as the SERS detection limit.

The selectivity of As^{3+} detection was verified by examining other metals (aluminum, cobalt, iron, potassium, nickel, lead and zinc). None of them yielded SERS signal comparable to arsenic (Fig. S4, Supporting Information). Additionally, spike and recovery experiments were carried out for three different concentrations of As^{3+} in tap water using the GSH + 2-MPY modified AgNPs. Table S3 (Supporting Information) presents the recovery rates, which are nearly 100%, suggesting excellent selectivity of this method in detecting As^{3+}.

4. Conclusions

In an effort to develop simple, selective and sensitive As^{3+} detection, we utilized colloid aggregation aided by cross-linking between arsenic and glutathione. SERS of three mercapto-compounds was monitored. In the presence of As^{3+} and glutathione, the SERS signal of 2-MPY was very strongly enhanced. We refer to this phenomenon as "aggregation-aided SERS" (AA-SERS). The suggested SERS enhancement mechanism is supported by UV–Vis absorption spectra, TEM and Raman imaging. Using this protocol, we did a concentration dependent study of As^{3+} ions in aqueous solution and attempted to detect the lowest concentration of arsenite ions possible. The novel use of 2-mercaptopyridine (2-MPY) made it possible to reach the lowest detection limit of As^{3+} (~0.5 ppb) achieved so far by the SERS technique. Our protocol represents efficient *direct* sensing of arsenite ions. Compared to other techniques, the method is relatively simple and does not rely on data extrapolation. We thus believe that it is of potential use in monitoring arsenic contamination of the environment.

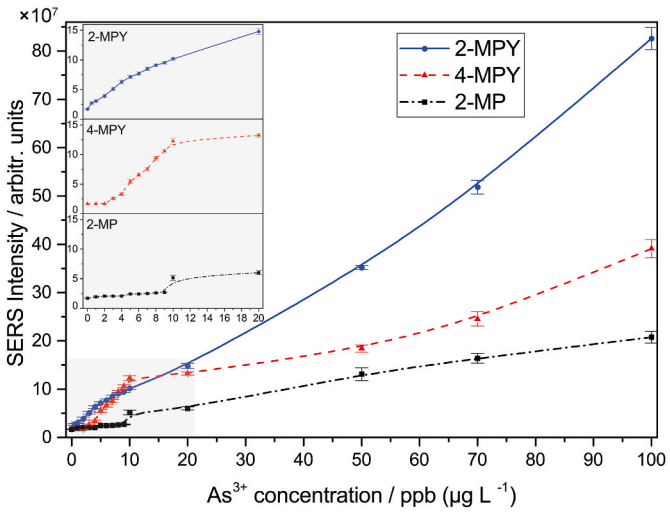

Fig. 7. Raman intensity of pyridine/pyrimidine ring breathing mode at ~1000 cm^{-1} for the three mercapto-compounds, as a function of As^{3+} concentration. Silver nanoparticles (AgNPs, nominally 0.25 mM $AgNO_3$) and glutathione (GSH, 0.5 µM) are also present. The errors bars depict standard deviations obtained from six independent spectra.

Credit author statement

Moumita Das: Conceptualization, Methodology, Investigation, Data curation, Writing – original draft. **Debraj Gangopadhyay:** Conceptualization, Methodology, Validation, Investigation, Writing – original draft, Writing – review & editing, Visualization. **Radek Pelc**: Methodology, Writing – review & editing. **Romana Hadravová**: Methodology. **Jaroslav Šebestík**: Methodology. **Petr Bouř**: Validation, Writing – review & editing, Visualization, Supervision, Project administration, Funding acquisition.

Declaration of competing interest

The authors declare that they have no known competing financial interests or personal relationships that could have appeared to influence the work reported in this paper.

Data availability

No data was used for the research described in the article.

Acknowledgments

The present study was supported by the European Regional Development Fund
(CZ.02.1.01/0.0/0.0/16_019/0000729) and the Czech Science Foundation (22-04669S).

Appendix A. Supplementary data

Supplementary data to this article can be found online at https://doi.org/10.1016/j.talanta.2022.123940.

References

[1] L. Chen, N. Zhou, J. Li, Z. Chen, C. Liao, J. Chen, Synergy of glutathione, dithiothreitol and N-acetyl-L-cysteine self-assembled monolayers for electrochemical assay: sensitive determination of arsenic (III) in environmental and drinking water, Analyst 136 (21) (2011) 4526–4532.
[2] A.H. Smith, C. Hopenhayn-Rich, M.N. Bates, H.M. Goeden, I. Hertz-Picciotto, H. M. Duggan, R. Wood, M.J. Kosnett, M.T. Smith, Cancer risks from arsenic in drinking water, Environ. Health Perspect. 97 (1992) 259–267.
[3] M. Hendryx, Mortality from heart, respiratory, and kidney disease in coal mining areas of Appalachia, Int. Arch. Occup. Environ. Health 82 (2) (2009) 243–249.
[4] H.-Y. Chiou, W.-I. Huang, C.-L. Su, S.-F. Chang, Y.-H. Hsu, C.-J. Chen, Dose-response relationship between prevalence of cerebrovascular disease and ingested inorganic arsenic, Stroke 28 (9) (1997) 1717–1723.
[5] A. Navas-Acien, E.K. Silbergeld, R. Pastor-Barriuso, E. Guallar, Arsenic exposure and prevalence of type 2 diabetes in US adults, JAMA 300 (7) (2008) 814–822.
[6] M.L. Kile, D.C. Christiani, Environmental arsenic exposure and diabetes, JAMA 300 (7) (2008) 845–846.
[7] B.K. Mandal, K.T. Suzuki, Arsenic round the world: a review, Talanta 58 (1) (2002) 201–235.
[8] A.A. Ensafi, A.C. Ring, I. Fritsch, Highly sensitive voltammetric speciation and determination of inorganic arsenic in water and alloy samples using ammonium 2-amino-1-cyclopentene-1-dithiocarboxylate, Electroanalysis: Int. J. Devoted Fund. Practical Aspect. Electroanalysis 22 (11) (2010) 1175–1185.
[9] S.J. Flora, Arsenic-induced oxidative stress and its reversibility following combined administration of n-acetylcysteine and meso 2, 3–dimercaptosuccinic acid in rats, Clin. Exp. Pharmacol. Physiol. 26 (11) (1999) 865–869.
[10] P. Rebuzzini, E. Cebral, L. Fassina, C.A. Redi, M. Zuccotti, S. Garagna, Arsenic trioxide alters the differentiation of mouse embryonic stem cell into cardiomyocytes, Sci. Rep. 5 (1) (2015) 1–10.
[11] A. Santra, A. Chowdhury, S. Ghatak, A. Biswas, G.K. Dhali, Arsenic induces apoptosis in mouse liver is mitochondria dependent and is abrogated by N-acetylcysteine, Toxicol. Appl. Pharmacol. 220 (2) (2007) 146–155.
[12] S.J. Flora, S. Chouhan, G.M. Kannan, M. Mittal, H. Swarnkar, Combined administration of taurine and monoisoamyl DMSA protects arsenic induced oxidative injury in rats, Oxid. Med. Cell. Longev. 1 (1) (2008) 39–45.
[13] D.S. Martin, S.E. Willis, D.M. Cline, N-acetylcysteine in the treatment of human arsenic poisoning, J. Am. Board Fam. Pract. 3 (4) (1990) 293–296.
[14] S. Shen, X.-F. Li, W.R. Cullen, M. Weinfeld, X.C. Le, Arsenic binding to proteins, Chem. Rev. 113 (10) (2013) 7769–7792.
[15] B. Chen, Q. Liu, A. Popowich, S. Shen, X. Yan, Q. Zhang, X.-F. Li, M. Weinfeld, W. R. Cullen, X.C. Le, Therapeutic and analytical applications of arsenic binding to proteins, Metallomics 7 (1) (2015) 39–55.
[16] M. Das, K.K. Singh, E. Khan, R.K. Sinha, R.K. Singh, P. Tandon, D. Gangopadhyay, N-Acetylcysteine versus arsenic poisoning: a mechanistic study of complexation by molecular spectroscopy and density functional theory, J. Mol. Liq. 340 (2021), 117168.
[17] F. Parvez, Y. Chen, M. Argos, A.I. Hussain, H. Momotaj, R. Dhar, A. van Geen, J. H. Graziano, H. Ahsan, Prevalence of arsenic exposure from drinking water and awareness of its health risks in a Bangladeshi population: results from a large population-based study, Environ. Health Perspect. 114 (3) (2006) 355–359.
[18] D.G. Mazumder, Effect of chronic intake of arsenic-contaminated water on liver, Toxicol. Appl. Pharmacol. 206 (2) (2005) 169–175.
[19] A. Heikens, Arsenic Contamination of Irrigation Water, Soil and Crops in Bangladesh: Risk Implications for Sustainable Agriculture and Food Safety in Asia, Rap Publication (FAO), 2006.
[20] P.L. Smedley, D.G. Kinniburgh, A review of the source, behaviour and distribution of arsenic in natural waters, Appl. Geochem. 17 (5) (2002) 517–568.
[21] M.F. Naujokas, B. Anderson, H. Ahsan, H.V. Aposhian, J.H. Graziano, C. Thompson, W.A. Suk, The broad scope of health effects from chronic arsenic exposure: update on a worldwide public health problem, Environ. Health Perspect. 121 (3) (2013) 295–302.
[22] J. Hao, M.-J. Han, S. Han, X. Meng, T.-L. Su, Q.K. Wang, SERS detection of arsenic in water: a review, J. Environ. Sci. 36 (2015) 152–162.
[23] N. Deedar, I. Aslam, Evaluation of the adsorption potential of titanium dioxide nanoparticles for arsenic removal, J. Environ. Sci. 21 (3) (2009) 402–408.
[24] P. Wang, G. Sun, Y. Jia, A.A. Meharg, Y. Zhu, A review on completing arsenic biogeochemical cycle: microbial volatilization of arsines in environment, J. Environ. Sci. 26 (2) (2014) 371–381.
[25] D.v. Halem, S. Bakker, G. Amy, J. Van Dijk, Arsenic in drinking water: a worldwide water quality concern for water supply companies, Drink. Water Eng. Sci. 2 (1) (2009) 29–34.
[26] E.F.S. Authority, D. Arcella, C. Cascio, J.Á. Gómez Ruiz, Chronic dietary exposure to inorganic arsenic, EFSA J. 19 (1) (2021), e06380.
[27] F. Cubadda, M. D'Amato, F. Mancini, F. Aureli, A. Raggi, L. Busani, A. Mantovani, Assessing human exposure to inorganic arsenic in high-arsenic areas of Latium: a biomonitoring study integrated with indicators of dietary intake, Ann Ig 27 (1) (2015) 39–51.
[28] A.-L. Lindberg, W. Goessler, E. Gurzau, K. Koppova, P. Rudnai, R. Kumar, T. Fletcher, G. Leonardi, K. Slotova, E. Gheorghiu, Arsenic exposure in Hungary, Romania and Slovakia, J. Environ. Monit. 8 (1) (2006) 203–208.
[29] H.A. Rowland, E.O. Omoregie, R. Millot, C. Jimenez, J. Mertens, C. Baciu, S.J. Hug, M. Berg, Geochemistry and arsenic behaviour in groundwater resources of the Pannonian Basin (Hungary and Romania), Appl. Geochem. 26 (1) (2011) 1–17.
[30] D. Middleton, M. Watts, E. Hamilton, E. Ander, R. Close, K. Exley, H. Crabbe, G. Leonardi, T. Fletcher, D. Polya, Urinary arsenic profiles reveal exposures to inorganic arsenic from private drinking water supplies in Cornwall, UK, Sci. Rep. 6 (1) (2016) 1–11.
[31] I. Herath, M. Vithanage, J. Bundschuh, J.P. Maity, P. Bhattacharya, Natural arsenic in global groundwaters: distribution and geochemical triggers for mobilization, Current Pollution Reports 2 (1) (2016) 68–89.
[32] T.J. Sorg, A.S. Chen, L. Wang, Arsenic species in drinking water wells in the USA with high arsenic concentrations, Water Res. 48 (2014) 156–169.

[33] M. Mulvihill, A. Tao, K. Benjauthrit, J. Arnold, P. Yang, Surface-enhanced Raman spectroscopy for trace arsenic detection in contaminated water, Angew. Chem. Int. Ed. 47 (34) (2008) 6456–6460.
[34] J. Li, L. Chen, T. Lou, Y. Wang, Highly sensitive SERS detection of As3+ ions in aqueous media using glutathione functionalized silver nanoparticles, ACS Appl. Mater. Interfaces 3 (10) (2011) 3936–3941.
[35] N. Qi, B. Li, H. You, W. Zhang, L. Fu, Y. Wang, L. Chen, Surface-enhanced Raman scattering on a zigzag microfluidic chip: towards high-sensitivity detection of as (III) ions, Anal. Methods 6 (12) (2014) 4077–4082.
[36] L. Chen, X. Fu, J. Li, Ultrasensitive surface-enhanced Raman scattering detection of trypsin based on anti-aggregation of 4-mercaptopyridine-functionalized silver nanoparticles: an optical sensing platform toward proteases, Nanoscale 5 (13) (2013) 5905–5911.
[37] T.S. Choong, T. Chuah, Y. Robiah, F.G. Koay, I. Azni, Arsenic toxicity, health hazards and removal techniques from water: an overview, Desalination 217 (1–3) (2007) 139–166.
[38] C. Moscoso-Pérez, J. Moreda-Piñeiro, P. López-Mahía, S. Muniategui-Lorenzo, E. Fernández-Fernández, D. Prada-Rodríguez, Pressurized liquid extraction followed by high performance liquid chromatography coupled to hydride generation atomic fluorescence spectrometry for arsenic and selenium speciation in atmospheric particulate matter, J. Chromatogr. A 1215 (1–2) (2008) 15–20.
[39] N. Zhang, N. Fu, Z. Fang, Y. Feng, L. Ke, Simultaneous multi-channel hydride generation atomic fluorescence spectrometry determination of arsenic, bismuth, tellurium and selenium in tea leaves, Food Chem. 124 (3) (2011) 1185–1188.
[40] S. Kempahanumakkagari, A. Deep, K.-H. Kim, S.K. Kailasa, H.-O. Yoon, Nanomaterial-based electrochemical sensors for arsenic-A review, Biosens. Bioelectron. 95 (2017) 106–116.
[41] G. Bhanjana, N. Dilbaghi, S. Chaudhary, K.-H. Kim, S. Kumar, Robust and direct electrochemical sensing of arsenic using zirconia nanocubes, Analyst 141 (13) (2016) 4211–4218.
[42] K. Jitmanee, M. Oshima, S. Motomizu, Speciation of arsenic (III) and arsenic (V) by inductively coupled plasma-atomic emission spectrometry coupled with preconcentration system, Talanta 66 (3) (2005) 529–533.
[43] K. Mao, H. Zhang, Z. Wang, H. Cao, K. Zhang, X. Li, Z. Yang, Nanomaterial-based aptamer sensors for arsenic detection, Biosens. Bioelectron. 148 (2020), 111785.
[44] D.L. Jeanmaire, R.P. Van Duyne, Surface Raman spectroelectrochemistry: Part I. Heterocyclic, aromatic, and aliphatic amines adsorbed on the anodized silver electrode, J. Electroanal. Chem. Interfacial Electrochem. 84 (1) (1977) 1–20.
[45] M. Moskovits, Surface-enhanced spectroscopy, Rev. Mod. Phys. 57 (3) (1985) 783.
[46] K.C. Bantz, A.F. Meyer, N.J. Wittenberg, H. Im, Ö. Kurtuluş, S.H. Lee, N. C. Lindquist, S.-H. Oh, C.L. Haynes, Recent progress in SERS biosensing, Phys. Chem. Chem. Phys. 13 (24) (2011) 11551–11567.
[47] H. Li, X. Wang, Z. Wang, J. Jiang, Y. Qiao, M. Wei, Y. Yan, C. Li, A high-performance SERS-imprinted sensor doped with silver particles of different surface morphologies for selective detection of pyrethroids in rivers, New J. Chem. 41 (23) (2017) 14342–14350.
[48] J.-F. Li, Y.-J. Zhang, S.-Y. Ding, R. Panneerselvam, Z.-Q. Tian, Core–shell nanoparticle-enhanced Raman spectroscopy, Chem. Rev. 117 (7) (2017) 5002–5069.
[49] B. Sharma, R.R. Frontiera, A.-I. Henry, E. Ringe, R.P. Van Duyne, SERS: materials, applications, and the future, Mater. Today 15 (1–2) (2012) 16–25.
[50] Z. Chen, S. Luo, C. Liu, Q. Cai, Simple and sensitive colorimetric detection of cysteine based on ssDNA-stabilized gold nanoparticles, Anal. Bioanal. Chem. 395 (2) (2009) 489–494.
[51] D. Gangopadhyay, P. Sharma, R. Nandi, M. Das, S. Ghosh, R.K. Singh, In vitro concentration dependent detection of creatinine: a surface enhanced Raman scattering and fluorescence study, RSC Adv. 6 (113) (2016) 112562–112567.
[52] W.A. El-Said, H.-Y. Cho, J.-W. Choi, SERS Application for Analysis of Live Single Cell, Nanoplasmonics - Fundamentals and Applications, London, United Kingdom, 2017. IntechOpen.
[53] S.J. Greaves, W.P. Griffith, Surface-enhanced Raman spectroscopy (SERS) of ligands and their complexes on silver sols—I. Maltol, tropolone and their complexes with group VIII and group VI metals, Polyhedron 7 (19–20) (1988) 1973–1979.
[54] J.R. Kalluri, T. Arbneshi, S. Afrin Khan, A. Neely, P. Candice, B. Varisli, M. Washington, S. McAfee, B. Robinson, S. Banerjee, Use of gold nanoparticles in a simple colorimetric and ultrasensitive dynamic light scattering assay: selective detection of arsenic in groundwater, Angew. Chem. 121 (51) (2009) 9848–9851.
[55] Z. Xu, J. Hao, F. Li, X. Meng, Surface-enhanced Raman spectroscopy of arsenate and arsenite using Ag nanofilm prepared by modified mirror reaction, J. Colloid Interface Sci. 347 (1) (2010) 90–95.
[56] L. Song, K. Mao, X. Zhou, J. Hu, A novel biosensor based on Au@ Ag core–shell nanoparticles for SERS detection of arsenic (III), Talanta 146 (2016) 285–290.
[57] R. Liu, J.-f. Sun, D. Cao, L.-q. Zhang, J.-f. Liu, G.-b. Jiang, Fabrication of highly-specific SERS substrates by co-precipitation of functional nanomaterials during the self-sedimentation of silver nanowires into a nanoporous film, Chem. Commun. 51 (7) (2015) 1309–1312.
[58] A. Michota, J. Bukowska, Surface-enhanced Raman scattering (SERS) of 4-mercaptobenzoic acid on silver and gold substrates, J. Raman Spectrosc. 34 (1) (2003) 21–25.
[59] L. Mulfinger, S.D. Solomon, M. Bahadory, A.V. Jeyarajasingam, S.A. Rutkowsky, C. Boritz, Synthesis and study of silver nanoparticles, J. Chem. Educ. 84 (2) (2007) 322.
[60] M. Das, D. Gangopadhyay, J. Šebestík, L. Habartová, P. Michal, J. Kapitán, P. Bouř, Chiral detection by induced surface-enhanced Raman optical activity, Chem. Commun. 57 (52) (2021) 6388–6391.
[61] P. Niederhafner, M. Šafařík, J. Neburková, T.A. Keiderling, P. Bouř, J. Šebestík, Monitoring peptide tyrosine nitration by spectroscopic methods, Amino Acids 53 (4) (2021) 517–532.
[62] M.F. Hamissa, P. Niederhafner, H. Šestáková, M. Šafařík, R. Hadravová, J. Šebestík, Neutral and charged forms of inubosin B in aqueous solutions at different pH and on the surface of Ag nanoparticles, J. Mol. Struct. 1250 (2022), 131828.
[63] L. Mo, D. Liu, W. Li, L. Li, L. Wang, X. Zhou, Effects of dodecylamine and dodecanethiol on the conductive properties of nano-Ag films, Appl. Surf. Sci. 257 (13) (2011) 5746–5753.
[64] K.L. Wustholz, A.-I. Henry, J.M. McMahon, R.G. Freeman, N. Valley, M.E. Piotti, M. J. Natan, G.C. Schatz, R.P. Van Duyne, Structure−Activity relationships in gold nanoparticle dimers and trimers for surface-enhanced Raman spectroscopy, J. Am. Chem. Soc. 132 (31) (2010) 10903–10910.
[65] R. Gill, L. Tian, H. van Amerongen, V. Subramaniam, Emission enhancement and lifetime modification of phosphorescence on silver nanoparticle aggregates, Phys. Chem. Chem. Phys. 15 (38) (2013) 15734–15739.